Advanced Journal of Chemistry-Section A

Journal homepage: www.ajchem-a.com

Original Research Article

Thermodynamic and Exergy Analysis of Cogeneration Cycles of Electricity and Heat Integrated with a Solid Oxide Fuel Cell Unit

Nima Norouzi*

Department of Energy Engineering and Physics, Amirkabir University of Technology (Tehran Polytechnic), 424 Hafez Avenue, PO. Box 15875-4413, Tehran, Iran

ARTICLE INFO

Article history

Submitted: 27 April 2021
Revised: 18 May 2021
Accepted: 31 May 2021
Available online: 05 June 2021
Manuscript ID: AJCA-2104-1255

DOI: 10.22034/AJCA.2021.283638.1255

KEYWORDS

SOFC
Cogeneration
CHP
Exergy analysis

ABSTRACT

Among the items that have been widely used as a solution to reduce energy consumption and air pollution are cycles of simultaneous generation of electricity and heat or CHP. In such cycles, the gas turbine's exhaust gases enter the steam production unit to produce the required steam or hot water. In the meantime, and due to the increasing use of oxidized fuel cells, combined circuits including fuel cells, gas turbines, and recovery boilers have been considered. In this paper, the combined cycle, including fuel, gas turbine, and recovery boiler, was thermodynamically analyzed, and its performance results are compared with a normal CHP cycle. Electrochemical and chemical modeling of fuel cells and exergy and thermodynamic analysis of all cycle components have been performed. In the cycle, performance changes with basic cycle parameters such as the temperature of the combustion products entering the gas turbine, the boiler steam pressure, the pinch point, the flow intensity, and the fuel cell stack temperature were analyzed. According to the results, the efficiency of the combined cycle with a fuel cell, is much higher, 61% compared with the 50% of the normal CHP.

GRAPHICAL ABSTRACT

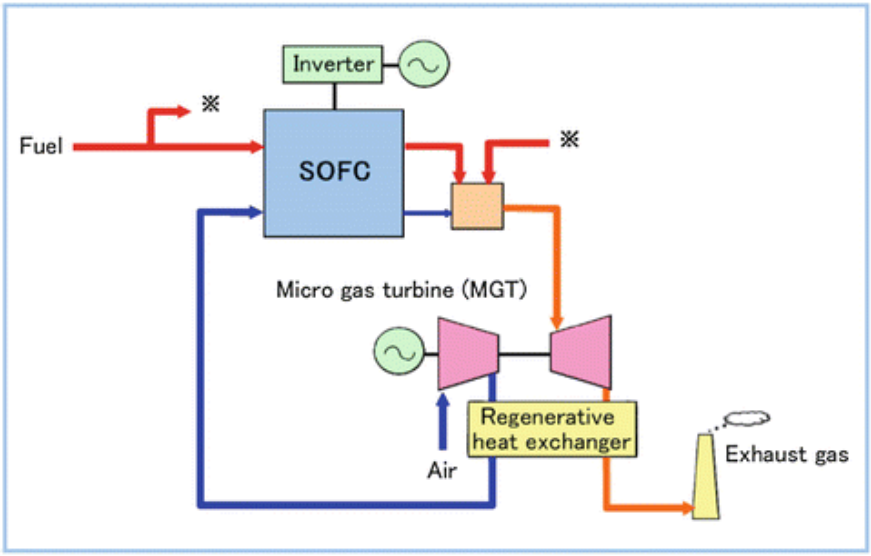

* Corresponding author: Norouzi, Nima
✉ E-mail: nima1376@aut.ac.ir

Introduction

The energy crisis in the present age is one of the fundamental challenges facing human beings today. Increasing energy consumption on the one hand and the importance of preserving the environment and increasing the price of energy carriers, on the other hand, has led to a tendency to use new methods of energy conversion and renewable energy sources. Fossil fuels are polluting, and their resources are limited, so the demand for fossil fuels in the world will exceed its production, which will lead to a crisis of energy shortage in the world.

Therefore, the use of alternative energy sources is essential [1-3]. According to the Kyoto Protocol provisions, energy-related industries will face the problem of finding a way to produce high-efficiency power and pay special attention to the environment and the optimal use of natural resources [4]. According to forecasts made by the International Energy Agency (IEA), most electricity generation in the future will be based on gas turbines. Therefore, achieving high-efficiency production technology, less pollution, and lower maintenance costs are essential for electricity generation. The use of gas turbines in modern cycles is one way to achieve this goal [5]. Also, as an efficient energy converter, fuel cells can be coupled with gas turbines and increase the efficiency of the hybrid system by 60%, while these turbines alone do not have efficiencies of more than 30%.[6]

The fuel cell is an electrochemical converter that converts the fuel and oxidizer's chemical energy directly into electrical energy and has no limitations on the Carnot cycle. The advantages of this technology can be low production of environmental pollutants, high efficiency compared with other technologies, power generation range from several watts to several megawatts, its use in various industries such as transportation, no moving parts, maintenance costs, and low noise pollution [7-9]. Among different types of fuel cells, solid oxide fuel cells, due to high operating temperatures, can direct use of light hydrocarbons, such as natural gas, and have a high potential for simultaneous production on medium to large scales.

The basic idea of a SOFC/ GT hybrid system is very simple. In fact, in a pressurized Brighton cycle, the fuel cell mass replaces the combustion chamber. SOFC/ GT hybrid cycles are usually powered by natural gas, and the natural gas in the fuel cell is converted to hydrogen-rich fuel by performing a series of chemical reactions. Internal fuel modification reduces system complexity and reduces the investment cost to build an ancillary fuel modification system [10-12]. However, the use of preliminary modifications increases the efficiency of the fuel cell mass. In this case, a small percentage of the input fuel (about 20%) is modified to start the fuel cell's electrochemical reactions as soon as the fuel enters the fuel cell mass. Otherwise, in the inlet sections of the anode cell, only the methane modification process is performed, and the rate of electrochemical reactions in the inlet section of the fuel cell is very low, which leads to a decrease in the efficiency of the fuel cell mass [13].

For internal fuel correction, there are two arrangements of direct internal correction and indirect internal correction. In the first type, the fuel in the fuel cell anode is directly converted to hydrogen-rich fuel. This type of layout simplifies the system and lowers investment costs. However, first, in this case it is necessary to perform the methane heater correction reaction and use a suitable catalyst in the fuel cell anode. Secondly, due to the large amounts of methane, the risk of carbon deposition on the fuel cell anode side is high. Thirdly, since the reaction of methane heater correction is very fast and endothermic, it significantly cools the fuel cell inlet parts, which creates a high-temperature gradient at the fuel cell inlet [8- 11, 13]. These problems may be alleviated by indirect internal

fuel correction in which the methane heater correction reaction takes place in a separate chamber because there is only one heat exchange between the modifier and the fuel cell. Indirect internal fuel modification leads to more complexity and higher investment costs [14, 15]. Various studies have been done in the field of hybrid systems, some of which are reviewed here.

Yang *et al*. [16] compared two fuel cell hybrid systems that used internal modification in one and external modification in the other. The first type had an indirect internal correction with a direct thermal connection with the cell, but the second type had an external correction that provides the correction process's heat through a converter. In this research, a comparison was made between two systems without a turbine, combustion chamber, and compressor. The results showed that the system's power generation capacity with internal modification was more than the one with external modification. Because in the type of internal modification, the ratio of air to fuel is less, and the airflow rate is assumed to be constant, more fuel reacts, and more power is produced. Later, two hybrid systems were compared for the same design parameters and the results showed that the system with internal modification required less fuel injection and therefore had higher efficiency.

To perform the methane heater correction reaction, steam is required [14, 15], and the first way to supply steam is to use hot gases leaving the system [10]. Due to the anode's electrochemical half-reaction, a certain amount of steam is produced in the fuel cell anode. Therefore, a possible alternative to the steam generator is to recirculate some of the anode exhaust gases using a high-temperature injector or blower into the fuel reform subsystem. Originally developed by Siemens and Settinghaus, this layout is the most common method due to its simplicity. Anode output recirculation reduces system costs and promises higher conversion efficiencies.

On the other hand, using a steam generator makes it easier to control the system because the amount of steam produced can be easily controlled [11, 13]. Zabihian and Fang [17] compared a SOFC / GT hybrid system with anode output recirculation with a steam generator. In this research, the fuel refining process was considered internally. A modifier was also been used to increase the rate of electrochemical reactions and prevent scale formation. The results showed that the system's overall electrical efficiency with anode recirculation was 74.6% and for the system with the steam generator was 73.9%. In a study, Granowski *et al*. [18] compared two fuel cell hybrid systems from the perspective of thermodynamics' first and second laws. In the first system, the anode and cathode outlets entered the combustion chamber, and the turbine outlet was used to preheat the air, fuel, and steam required by the correction process. Finally, in the coolant, the steam in the products was condensed and returned to the system as required. In the second system, some of the anode output was returned to its input for the correction process, and the rest entered the combustion chamber with the cathode output. Finally, the turbine output entered the steam generator to start the Rankin cycle and provides the required steam for the Rankin cycle. Based on the obtained results, the fuel consumption in the first system was higher, and as a result, its energy and exergy efficiency was lower than the second system, but the production capacity of the first system was more than the second system [19].

When the fuel cell is operating at ambient pressure, it must be indirectly coupled via a Brighton-cycle heat exchanger. This makes the work simple and easy and makes it easy to use fuels that cannot be used for fuel cells 2739 [19]. Park and Kim [20] compared two high-pressure and atmospheric SOFC/ GT systems. Their results

showed that the atmospheric system's efficiency was 5 to 10% lower than the high-pressure system. They also found a significant reduction in the turbine inlet temperature at higher pressure ratios, especially in the atmospheric system, which required additional air and fuel to be injected into the combustion chamber to control the turbine inlet temperature.

Direct SOFC/ GT hybrid systems have a complex thermal design. Because when the fuel cell operates at high temperatures, it is necessary to increase the air temperature entering the fuel cell with preheating because otherwise, the existence of a high thermal gradient in the fuel cell will cause serious damage. But when preheating is not sufficient due to the high compressor pressure ratio, the turbine's exhaust gases have a lower temperature, which causes the air temperature entering the fuel cell in the preheater not to increase much. To solve this problem, two combinations are used. In the first combination, the inlet air to the fuel cell is preheated using the combustion chamber exhaust gases. In this case, the temperature of the exhaust gases from the combustion chamber is higher, and as a result, the air temperature entering the fuel cell increases. This combination is completely different from the previously introduced systems because; in those systems, the turbine output is used for preheating.

On the other hand, because the temperature of the inlet gases to the turbine has decreased, the turbine's output power will be less. In the second composition, part of the combustion chamber outlet is combined with the inlet air and enters the fuel cell [19]. Zhang *et al*. [21] made a comparison between the two systems. Their results showed that the fuel cell's electrical efficiency in both systems was very close to each other, but because the output power of the turbine was lower in the first system, the overall electrical efficiency of the second system was significantly higher.

Fuel cells are good options for power generation due to their high efficiency and low pollution. Among the various fuel cells, solid oxide fuel cells are most commonly used, either alone or as part of a cycle. The combination of solid oxide fuel cell and the gas turbine is the most common and widespread combination used in power generation cycles with high efficiency and low pollution. Thermodynamic modeling of SOFC-GT cycles is the first step in investigating their performance. Different geometries and fuels are used in fuel cells. The type of fuel has significant effects on fuel cells' thermodynamic and environmental behavior [22-33].

It should be noted that it is necessary to use methane or natural gas to improve the process. Several different methods of fuel improvement are given in references [1]. To simulate the hybrid cycles of solid oxide fuel cell and gas turbine, it is necessary to study the chemical and electrochemical reactions and the relationships governing all the cycle components. Resources [2-4] have been used to obtain these relationships. The potential loss is in reference [3], and its details are in [4].

Methodology

Thermodynamic modeling of each system component

Figure 1 shows the schematic of the cycle. As it turns out, this cycle consists of a solid oxide fuel cell, a compressor, a gas turbine, a combustion chamber, and an air preheater**.**

In this modeling, natural gas with 97% methane, 1.5% carbon dioxide, 1.5% nitrogen [15, 17] and air with a combination of 79% nitrogen and 21% oxygen [4, 1] are considered. Therefore, chemical reactions, refining processes, and fuel upgrades must be considered. Table 1 shows the physical and electrochemical characteristics of the cell used.

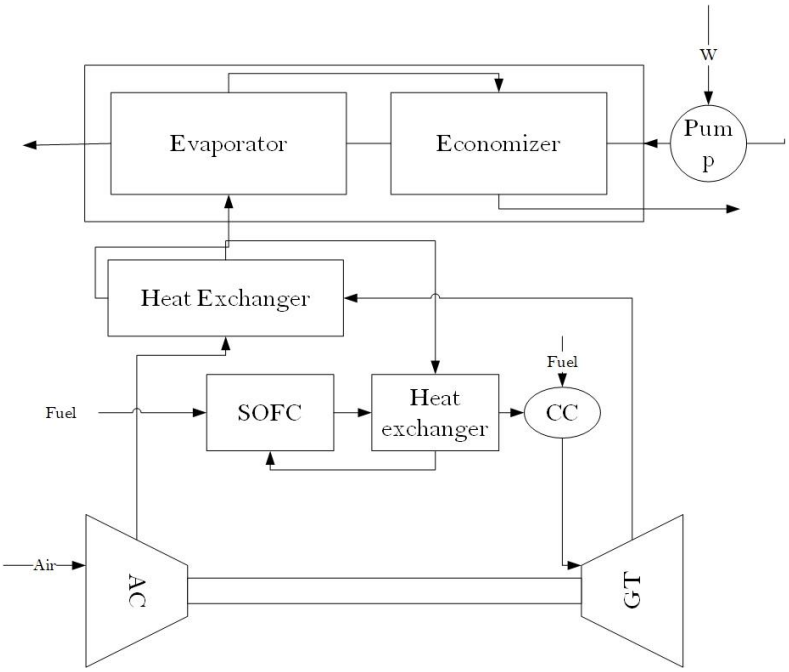

Figure 1. Schematic of the cycle

Table 1. Physical and electrochemical characteristics of the cell used [12]

Parameter	
Anode thickness (μm)	500
Cathode thickness (μm)	50
Electrolyte thickness (μm)	10
Effective area (cm^2)	100
Current density (A/cm^2)	0.2
Exchange current density in the anode	0.65
Exchange current density at the cathode	0.25

Mathematical Model

The solid oxide fuel cell is modeled based on the relationships and information in the reference [1] related to the tubular fuel cell. The equations for improving and upgrading the fuel are as follows:

$$CH_4 + H_2O \leftrightarrow H_2 + CO \quad (1)$$

$$CO + H_2O \leftrightarrow H_2 + CO_2 \quad (2)$$

The electrochemical reactions that generate heat and work are as follows:

$$H_2 + \frac{1}{2}O_2 \leftrightarrow H_2O \quad (3)$$

It should be noted that all chemical reactions are considered as equilibrium, and equilibrium constants are expressed by the following formulas [1, 8, 13]

$$K_{reforming} = \frac{x_{H_2}^2 x_{CO}}{x_{CH4} x_{H2O}} P^2 \quad (4)$$

$$K_{shifting} = \frac{x_{H2} x_{CO2}}{x_{CO} x_{H2O}} \quad (5)$$

$$lnK = AT^4 + BT^3 + CT^2 + DT + E \quad (6)$$

A, B, C, D are fixed values whose values are given in both modification and fuel upgrade in Table 2:

Table 2. Coefficients related to Equation 6 [10-13]

Constant	Reforming	Shifting
A	-2.6312e-11	5.47e-12
B	1.2406e-07	-2.5748e-08
C	-0.00022523	0.000046374
D	0.19503	-0.03915
E	-66.1395	13.2097

The ideal voltage of a fuel cell can be obtained by the Nernst equation as follows:

$$V_N = V_0 - \frac{RT}{2F}\ln\left(\frac{x_{H_2O}}{x_{H_2}\sqrt{x_{O_2}}}\right) \quad (7)$$

But due to the existing irreversibility, the fuel cell's actual voltage is lower than the Nernst voltage. These irreversibilities can be classified into three main groups: Significant losses, activation, and concentration. Therefore, the actual voltage of the cell is obtained as follows:

$$V = V_N - V_{ohm} - V_{act} - V_{con} \quad (8)$$

Significant potential loss can be obtained through the following equation [4, 3]:

$$V_{ohm} = (R_{contact} + \sum \rho_k L_k)_i \quad (9)$$

Wherein:

$$\rho_a = 8.114e-6\exp\left(\frac{600}{T}\right) \quad (10-1)$$

$$\rho_e = 2.94e-6\exp\left(\frac{10350}{T}\right) \quad (10-2)$$

$$\rho_c = 2.94e-6\exp\left(\frac{-1392}{T}\right) \quad (10-3)$$

$$\rho_i = 125.6e-6\exp\left(\frac{4690}{T}\right) \quad (10-4)$$

The amount of activation losses is obtained through the following equation [4]:

$$V_{act} = V_{act,a} + V_{act,c} = \frac{RT}{F}\sinh^{-1}\left(\frac{i}{2i_{o,a}}\right) + \frac{RT}{F}\sinh^{-1}\left(\frac{i}{2i_{o,c}}\right) \quad (11)$$

Concentration potential drop can be obtained as follows:

$$V_{con} = V_{con,a} + V_{con,c} = -\frac{RT}{2F}\left[ln\left(1-\frac{i}{i_{as}}\right) - \ln\left(1+\frac{x_{H2}i}{x_{H2O}i_{as}}\right)\right] + \frac{RT}{4F}ln\left(1-\frac{i}{i_{cs}}\right) \quad (12)$$

Current limitations at the anode and cathode are also given in reference [4, 3].

The output power of the fuel cell can be displayed as follows:

$$W_{FC} = IV \quad (13)$$

The thermodynamic model of the fuel cell is as follows:

$$\left(\sum_{anode} m_i h_i + \sum_{cathod} m_i h_i\right)_{in} = W_{FC} + \left(\left(\sum_{anode} m_i h_i + \sum_{cathod} m_i h_i\right)_{out} + Q_{FC} \quad (14)$$

Exergy losses for each part of the cycle are obtained from the following general relation:

$$E_D = Q\left(1 - \frac{T_0}{T}\right) - W + \sum_{in} E - \sum_{out} E \quad (15)$$

Where the exergy rate is equal to the total exergy rate and is as follows:

$$E = E_{ch} + E_{ph} \quad (16)$$

The thermodynamic model of air compressor is based on isentropic efficiency and compressor pressure ratio:

$$T_{out} = T_{in}\left(1 + \frac{1}{\eta_{AC}}\left[r_c^{\frac{\gamma_a - 1}{\gamma_a}} - 1\right]\right) \quad (17)$$

The equation for gas turbine modeling is as follows:

$$T_{out} = T_{in}\left(1 + \eta_{GT}\left[1 - \left(\frac{P_{in}}{P_{out}}\right)^{\frac{1-\gamma_g}{\gamma_g}}\right]\right) \quad (18)$$

In the combustion chamber, the fuel cell and natural gas exhaust gases react with each other. By the energy balance equations and the combustion equation, the molar flow rate of the combustion products and their temperature can be obtained.

The thermodynamic model of preheaters is written as follows:

$$\eta_{AP} m_g (h_{in} - h_{out})_g = m_a (h_{in} - h_{out})_a \quad (19)$$

Boyer heat recovery produces saturated vapor at a certain pressure (Pmain). The pinch point plays a key role in HRSG performance.

The following equations have been used to model HRSG:

$$T_{out} = T_{sat} + PP \quad (20)$$

$$m_{steam}(h_{out} - h_{in})_{steam} = m_g C_{Pg} (T_{in} - T_{out})_g \quad (21)$$

The following formulas obtain the net output work and the exergy efficiency of the whole cycle:

$$W_{net} = W_{FC} + W_{GT} - W_{AC} - W_{Pump} \quad (22)$$

$$\eta_{total} = \frac{W_{net} + E_{steam}}{1.06 m_{fuel} LHV} \quad (23)$$

Results and Discussion

In this chapter, a computer program in Matlab software was used to solve the equations. The written code can change the values of the parameters stated in Table 3 as desired. In this way, it is possible to examine the change of each parameter on the system performance.

Table 4 shows the list and range of changes of the parameters based on which the analysis is performed. Note that only one of these parameters will be changed when checking the system parameters. In this case, the values of the other parameters are considered constant. Thus, the stack temperature is 1000 ° C, and the compressor pressure ratio is 7.

Table 4. System analysis parameters and their range of changes

Parameter	Range
Stack temperature	900 - 1100
Pressure ratio	3 - 12

Before the parametric system was checked, the written code was checked with previous research results to determine its accuracy. Table 5 shows

the results obtained from the code for the solid oxide fuel cell's output voltage compared with the results presented in [4]. In the following table, we will examine the parametric system of the studied system.

Table 3. Values of input parameters of SOFC-MGT model [1]

SOFC	
Polytropic efficiency of air compressor	0.87
Isentropic efficiency of the fuel compressor	0.83
Effective surface, cm^2	834
Current density, A/cm^2	0.35
Fuel consumption factor (Uf)	0.85
Thabit Faraday	96487
Effective anode length, m	0.05
Effective cathode length, m	0.005
Effective electrolyte length, m	0.001
Number of single stack cells	1152
Gas Turbine	
Inlet gas temperature to turbine, °C	1127
Polytropic turbine efficiency	0.85

Table 5. Comparison of the results of the thermodynamic model with reference

Power density		**Fuel Cell voltage**		**Current density**
Ref [4]	**Current study**	**Ref [4]**	**Current study**	
0.083	0.081	0.830	0.797	0.1
0.159	0.157	0.794	0.786	0.2
0.226	0.230	0.754	0.766	0.3
0.282	0.292	0.705	0.730	0.4
0.319	0.350	0.639	0.701	0.5

Figure 2 shows the exergy losses of the various components of the simple GT cycle and the SOFC-GT cycle are compared. Chemical reactions are the most important exergy dissipators in power generation cycles, confirmed by the results: HRSG, combustion chamber, and fuel cell are the most exergy dissipators in the cycle [12].

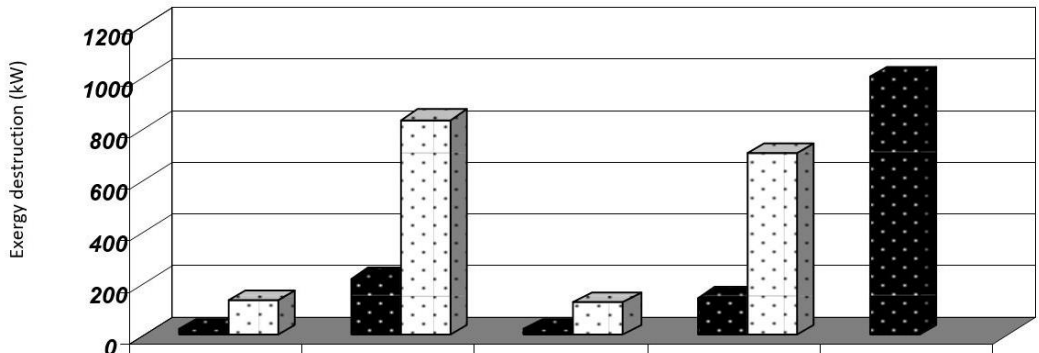

	Compressor	Combustion chamber	Gas Turbine	HRSG	SOFC
SOFCGTSG	24.97	220.27	24.36	145.24	1004.79
GTSG	133.87	836.45	126.47	707.06	

Figure 2. Comparison of exergy losses of different components of GTSG and SOFCGTSG cycles

Table 6 shows the simulation results of both GTSG and SOFCGTSG cycles. In this paper, the net output power of both cycles was considered equal. The exergy efficiency of the fuel cell was almost twice that of the gas turbine. Because of about 80% of the fuel cell's net output power, the exergy efficiency of the SOFCGTSG cycle increased. The SOFCGTSG exergy efficiency is also higher than the GTSG cycle, as shown in Table 6. The mass discharges of both cycles are compared. Comparing the mass flow rate of fuel in the two cases shows that the mass flow rate of fuel in the SOFCGTSG cycle is significantly lower than the GTSG cycle. Reducing fuel flow reduces carbon dioxide emissions as well as operating costs.

Table 6. Coefficients related to Equation 6 [10-13]

	SOFCGTSG	GTSG
Exergy efficiency	%61	%50
Fuel consumption in combustion chamber (kg/s)	0.02	0.13
Net cycle output power (kW)	2090.92	2090.92
Fuel cell power (kW)	1783.34	-
Inlet airflow to the fuel cell (kg/s)	1.36	-
Fuel cell inlet fuel flow rate (kg/s)	0.06	-
Airflow rate (kg /s)	-	7.28
Steam flow rate (kg /s)	0.31	1.53

In this section, we examine the effects of different parameters on cycle performance. Figure 3 shows the generated steam pressure on the generated steam's exergy efficiency and mass flow rate. As the steam pressure increases, the water's boiling temperature also increases, so more heat is needed to produce steam. Now, assuming the combustion products' condition inlet to the recycling boiler is constant, the steam flow output from the recycling boiler decreases with increasing steam pressure and reduces the temperature of the smoke coming out of the HRSG, which reduces the cycle exergy losses. In the heat transfer process, the temperature level

of heat transfer has an important effect on the rate of exergy degradation, so that the closer the heat transfer occurs at temperature levels closer to ambient temperature, the greater the rate of exergy degradation. Since increasing the steam pressure of the recovery boiler means increasing the boiling point of water and increasing the mean heat transfer in the boiler, the exergy degradation decreases, so the exergy efficiency increases.

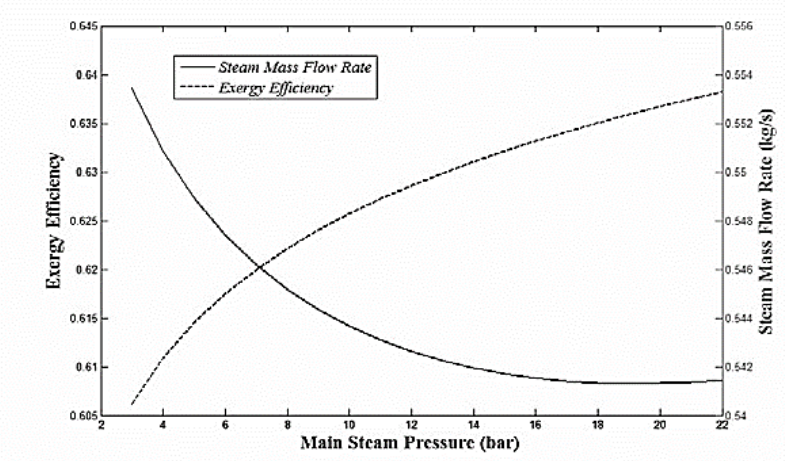

Figure 3. The effect of vapor pressure on the exergy efficiency and mass flow of steam

The effect of the pinch point on the exergy efficiency as well as steam production is shown in Figure 4. Increasing the pinch point increases the temperature of the smoke coming out of the turbine. As a result, the exergy efficiency and the rate of steam production are reduced. It is necessary to pay attention to the fact that reducing the pinch point's temperature requires increasing the heat transfer level in the exchanger, so the exchanger's price increases.

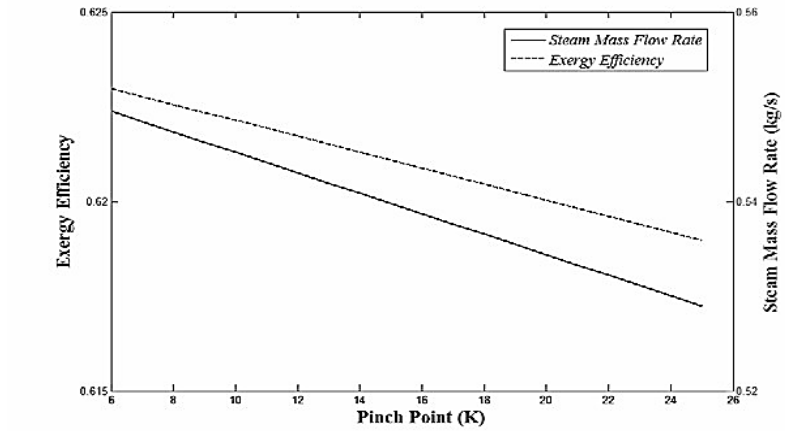

Figure 4. The effect of pinch point on the exergy efficiency and output steam output

Compressor pressure ratio has a significant effect on the gas turbine cycle. This effect is shown in Figure 5. The effect of compressor pressure ratio on the GT cycle is fully described in the articles.

As the inlet temperature to the gas turbine increases, the fuel inlet's mass flow rate to the combustion chamber also increases, as does the net output power of the GT cycle. Increasing the turbine power significantly reduces the exergy efficiency. High power generation reduces cycle efficiency. This effect is shown in Figure 6.

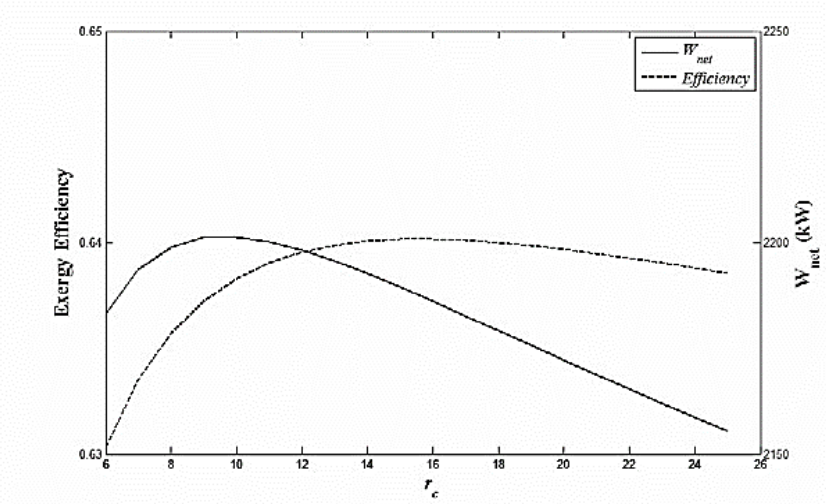

Figure 5. Changes in exergy efficiency and net output power with compressor pressure ratio

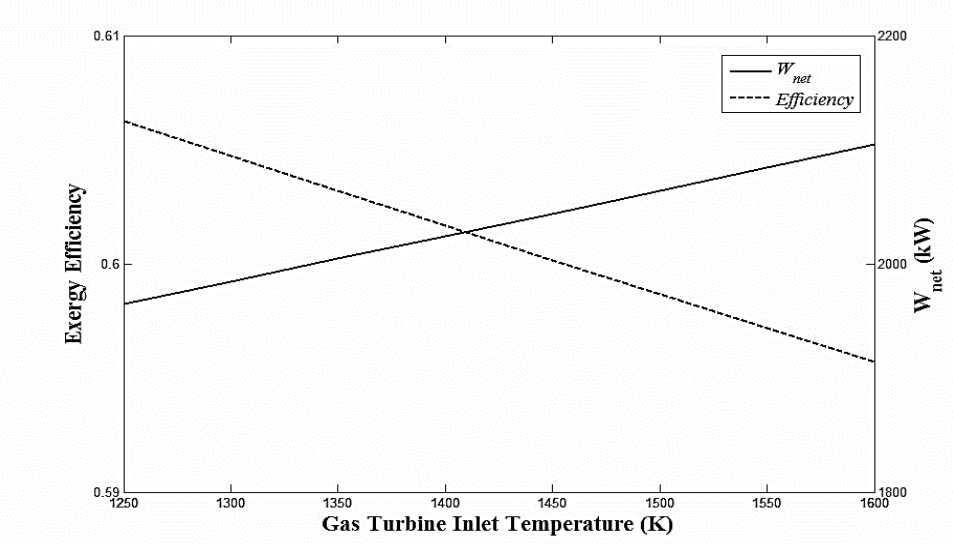

Figure 6. Effect of gas turbine inlet temperature on exergy efficiency and net output power

Fuel cell stack temperature is one of its important characteristics. The airflow rate can control the fuel cell stack temperature. The SOFC fuel flow rate is constant at a constant current density. As the fuel cell stack temperature increases, the SOFC exergy efficiency decreases due to increased activation and concentration losses. Besides, increasing the fuel cell stack's temperature leads to a decrease in the fuel rate of the fuel entering the combustion chamber, increasing the cycle's overall efficiency (Figure 7).

Increasing the current density reduces the SOFC efficiency, which ultimately reduces the total cycle exergy efficiency. Besides, the increase in current density is accompanied by an increase in the fuel flow inlet to the fuel cell, which increases the mass flow rate of the smoke entering the HRSG, so as shown in Figure 8, with increasing current density, the mass flow of steam also increases.

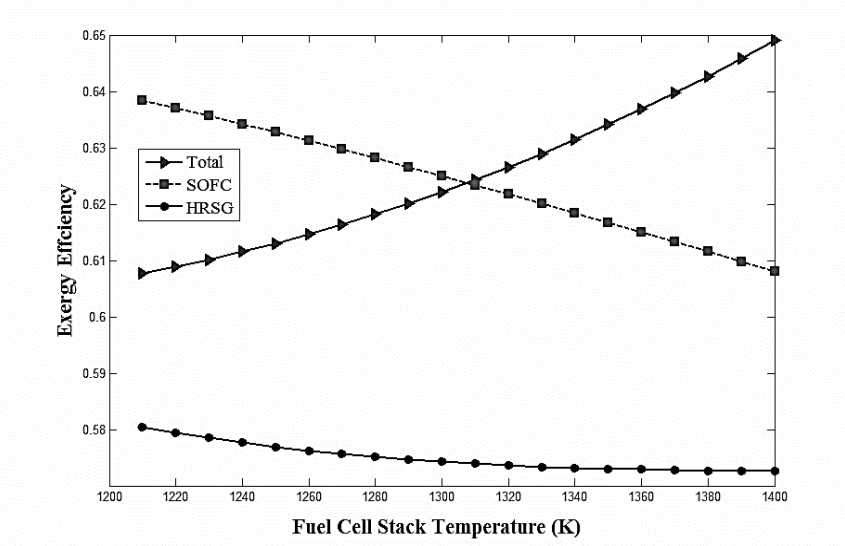

Figure 7. Exergy efficiency changes of important exergy wasters with fuel cell stack temperature

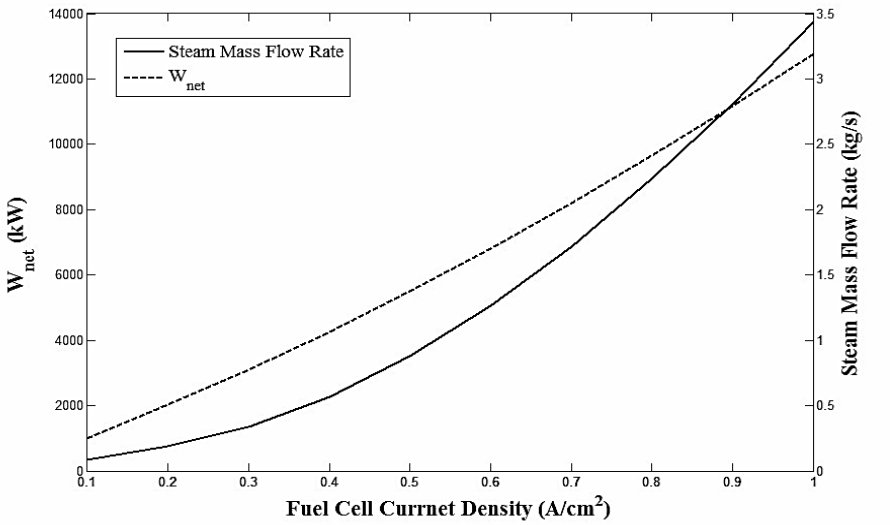

Figure 8. The effect of fuel cell current density on production capacity and steam output

Conclusion

In this research, a fuel cell hybrid system was purposefully selected and analyzed. Preliminary energy and exergy analysis results showed that the system's overall efficiency and exergy were 81.6% and 60.7%, respectively. The largest share of exergy degradation is related to the fuel cell mass, combustion chamber, and preliminary fuel modifier. The results of the parametric analysis indicate that:

- In a fuel unit, increasing pressure and temperature increases the fuel cell's power and efficiency, while in a hybrid system, the fuel cell shows dual behavior by increasing the system pressure because by overcoming the effect of temperature on pressure, the system's performance will decrease in increasing pressure, indicating that the fuel cell mass temperature cannot be constant.
- Increasing the fuel consumption coefficient increases the hybrid system's power and efficiency, and its optimal value is in the

range of 0.8 to 0.85. In a fuel cell mass, this range can be wider due to the high number.

- Increasing the steam ratio to carbon harms the fuel cell's power and efficiency, but the minimum amount must be observed to prevent carbon deposition.
- As the percentage of pretreatment increases, the hybrid system's power and efficiency increase until the concentration of reactants increases.

Given that the fuel cell has the largest share of power generation in the hybrid system, the system's net output power behaves similarly to the behavior of the cell's output power.

Acknowledgements

The authors are grateful for the scientific support from Amirkabir University.

Disclosure statement

No potential conflict of interest was reported by the author.

ORCID

Nima Norouzi : 0000-0002-2546-4288

References

[1] S. Park, T. Kim, *J. Power Sources*, **2006**, *163*, 490–499. [CrossRef], [Google Scholar], [Publisher]

[2] X. Zhang, S. Su, J. Chen, Y. Zhao, N. Brandon, *Int. J. Hydrogen Energy*, **2011**, *36*, 15304–15312. [CrossRef], [Google Scholar], [Publisher]

[3] M. Mortazaei, M. Rahimi, *J. Mech. Eng*. **2018**, *48*, 317–328. [Google Scholar], [Publisher]

[4] D. Singh, E. Hernández-Pacheco, P.N. Hutton, N. Patel, M.D. Mann, *J. Power Sources*, **2005**, *142*, 194–199. [CrossRef], [Google Scholar], [Publisher]

[5] A.G. Anastasiadis, S.A Konstantinopoulos, G.P. Kondylis, G.A. Vokas, P. Papageorgas, *Int. J. Hydrogen Energy*, **2017**, *42*, 3479–3486. [CrossRef], [Google Scholar], [Publisher]

[6] B. Najafi, A. Shirazi, M. Aminyavari, F. Rinaldi, R.A. Taylor, *Desalination* **2014**, *334*, 46–59. [CrossRef], [Google Scholar], [Publisher]

[7] H. Radmanesh, H. Hadi, *J. Model. Eng.*, **2019**, *16*, 411-426. [Google Scholar], [Publisher]

[8] N. Chatrattanawet, D. Saebea, S. Authayanun, A. Arpornwichanop, Y. Patcharavorachot, *Energy*, **2018**, *146*, 131–140. [CrossRef], [Google Scholar], [Publisher]

[9] K. Owebor, C.O.C. Oko, E.O. Diemuodeke, O.J. Ogorure, *Appl. Energy*, **2019**, *239*, 1385–1401. [CrossRef], [Google Scholar], [Publisher]

[10] D. Roy, S. Samanta, S. Ghosh, *J. Clean. Prod*., **2019**, *225*, 36–57. [CrossRef], [Google Scholar], [Publisher]

[11] G. Valencia, A. Benavides, Y. Cárdenas, *Energies*, **2019**, *12*, 2119. [CrossRef], [Google Scholar], [Publisher]

[12] P. Lisbona, J. Uche, L. Serra, *Desalination*, **2005**, *182*, 471–482. [CrossRef], [Google Scholar], [Publisher]

[13] V. Eveloy, P. Rodgers, L. Qiu, *Energy Convers. Manage*., **2016**, *126*, 944–959. [CrossRef], [Google Scholar], [Publisher]

[14] F. Ghirardo, M. Santin, A. Traverso, A. Massardo, *Int. J. Hydrogen Energy*, **2011**, *36*, 8134–8142. [CrossRef], [Google Scholar], [Publisher]

[15] H.A. Reyhani, M. Meratizaman, A. Ebrahimi, O. Pourali, M. Amidpour, Energy, **2016**, *107*, 141–164. [CrossRef], [Google Scholar], [Publisher]

[16] R. Ahmadi, S.M. Pourfatemi, S. Ghaffari, *Desalination*, **2017**, *411*, 76–88. [CrossRef], [Google Scholar], [Publisher]

[17] M. Hosseini, I. Dincer, P. Ahmadi, H.B. Avval, M. Ziaasharhagh, *Int. J. Energy Res*., **2013**, *37*, 426–434. [CrossRef], [Google Scholar], [Publisher]

[18] J. Beyrami, A. Chitsaz, K. Parham, Ø. Arild, *Energy*, **2019**, *186*, 115811. [CrossRef], [Google Scholar], [Publisher]

[19] S. Jehandideh, H. Hassanzade, S.E. Shakib, *Modares Mech. Eng*., **2019**, *19*, 2737–2749. [Google Scholar], [Publisher]

[20] J. Pirkandi, M. Mahmoodi, F. Amanloo, *Modares Mech. Eng*., **2015**, *15*, 132-144. [Google Scholar], [Publisher]

[21] M. Ni, *Int. J. Hydrogen Energy*, **2012**, *37*, 1731–1745. [CrossRef], [Google Scholar], [Publisher]

[22] C. Bao, Y. Wang, D. Feng, Z. Jiang, X. Zhang, *Progr. Energy Combust. Sci.*, **2018**, *66*, 83–140. [CrossRef], [Google Scholar], [Publisher]

[23] J. Pirkandi, M. Chassemi, M. Hamedi, *Fuel and Combustion* **2012**, 4(2): 67–89. [Google Scholar], [Publisher]

[24] A. Shirazi, B. Najafi, M. Aminyavari, F. Rinaldi, R.A. Taylor, *Energy*, **2014**, *69*, 212–226. [CrossRef], [Google Scholar], [Publisher]

[25] M.A. Farzad, H. Hassanzadeh, A. Safavinejad, M.R. Agaebrahimi, *J. Solid Fluid Mech.,* **2016**, *5*, 213–228. [CrossRef], [Google Scholar], [Publisher]

[26] S.H. Chan, C.F. Low, O.L. Ding, *J. Power Sources*, **2002**, *103*, 188–200. [CrossRef], [Google Scholar], [Publisher]

[27] A. Esmaieli, M.P. Keshavarz S.E. Shakib, M. Amidpour, *Int. J. Energy Res*., **2013**, *37*, 1440–1452. [CrossRef], [Google Scholar], [Publisher]

[28] H.T. El-Dessouky, H.M. Ettouney, Fundamentals of salt water desalination. Amsterdam: Elsevier, **2002**. [Google Scholar]

[29] S.E. Shakib, M. Amidpour, C. Aghanajafi, *Desalination*, **2012**, 285, 366–376. [CrossRef], [Google Scholar], [Publisher]

[30] R.B. Power, Steam jet ejectors for the process industries [glossary included]. Mc Graw-hill, **1994**. [Google Scholar]

[31] P. Ahmadi, I. Dincer, *Energy*, **2010**, *35*, 5161–5172. [CrossRef], [Google Scholar], [Publisher]

[32] J. Pirkandi, M. Chassemi, M.H. Hamedi, *Modares Mech. Eng*., **2012**, *12*, 117–133. [Google Scholar], [Publisher]

[33] M. Shakouri, H. Ghadamian, R. Sheikholeslami, *Desalination*, **2010**, *260*, 254–263. [CrossRef], [Google Scholar], [Publisher]

HOW TO CITE THIS ARTICLE

Nima Norouzi. Thermodynamic and Exergy Analysis of Cogeneration Cycles of Electricity and Heat Integrated with a Solid Oxide Fuel Cell Unit. *Adv. J. Chem. A*, **2021**, 4(4), 244-257.

DOI: 10.22034/AJCA.2021.283638.1255
URL: http://www.ajchem-a.com/article_131440.html